Supplementary Information

Enhanced Migration of Human Gingival Fibroblasts via Non-Thermal Biocompatible Dielectric Barrier Discharge Plasma

Ihn Han[1.2¶], In-Seok Song[3¶], Seung Ah Choi[4], Taebok Lee[5], Maksudbek Yusupov[6], Priyanka Shaw[6], Annemie Bogaerts[6], Eun Ha Choi[1*], and Jae Jun Ryu[3*]

[1]Plasma Bioscience Research Center, Applied Plasma Medicine Center, Kwangwoon University, Seoul, 01897, Republic of Korea

[2]Department of Plasma Bio-Display, Kwangwoon University, Seoul 01897, Korea

[3]Department of Dentistry, Korea University Anam Hospital, Seoul, 02841, Republic of Korea

[4]Division of Pediatric Neurosurgery, Pediatric Clinical Neuroscience Center, Seoul National University Children's Hospital, Seoul, 03080, Republic of Korea.

[5]Confocal Core Facility, Center for Medical Innovation, Seoul National University Hospital, Seoul 03082, Korea

[6]Research group PLASMANT, Department of Chemistry, University of Antwerp, Universiteitsplein 1, B-2610 Antwerp, Belgium

[*]Corresponding author: Eun Ha Choi, Ph.D.

Plasma Bioscience Research Center, Kwangwoon University, Gwangun-ro 20, Nowon-gu, Seoul, 139-701, Republic of Korea, Tel.: +82-2-940-5661, Fax: +82-2-960-5664; E-mail: ehchoi@kw.ac.kr

[*]Corresponding author: Jae Jun Ryu, DDS, MSD, PhD

Department of Prosthodontics, Korea University Anam Hospital, 73, Inchon-ro, Seongbuk-gu, Seoul, 02841, Republic of Korea, Tel.: +82-2-920-5423, Fax: +82-2-921-7348; E-mail: koprosth@unitel.co.kr

¶ These authors contributed equally to this work.

Index of figure and table

1. Supplementary materials and methods

1.1 Quantification of gene expression

The PCR amplification programme consisted of an initial denaturation at 95 °C for 3 min, followed by 45 cycles of denaturation at 95 °C for 10 s, annealing at 60 °C for 30 s, and extension at 72 °C for 10 s. The following primers were used: for MMP-2, forward, 5′-AAGAAGTAGCTGTGACCGCC -3′, and reverse, 5′- TTGCTGGAGACAAATTCTGG -3′; for VEGF, forward, 5′-CACACAGGATGGCTTGAAGA-3′, and reverse, 5′- AGGGCAGAATCATCACGAAG -3′; for Collagen type I, forward, 5′-CACACGTCTCGGTCATGGTA-3′, and reverse, 5′-AAGAGGAAGGCCAAGTCGAG -3′; for Collagen type IV, forward, 5′-

CTCCACGAGGAGCACAGC-3′, reverse, 5′-CCTTTTGTCCCTTCACTCCA-3′; for PDGF-beta, forward, 5′-CTGGCATGCAAGTGTGAGAC-3′, reverse, 5′-AATGGTCACCCGAGTTTGG-3′; for CDKN1A (p21), forward, 5′-AGTCAGTTCCTTGTGGAGCC-3′, and reverse, 5′-CATGGGTTCTGACGGACAT-3′; and for beta-actin, forward, 5′-CCTTGCACATGCCGGAG-3′, and reverse, 5′-GCACAGAGCCTCGCCTT -3′.

1.2 Immunoblot analysis

Briefly, total protein concentration in cell lysates was determined using the Pierce BCA Protein Assay Kit (Thermo Fisher Scientific, MA, USA). An equal amount of total protein (20 µg) was loaded on a (4–12) % gradient SDS-polyacrylamide gel for electrophoresis. The proteins were transferred onto a nitrocellulose membrane (Amersham™ Protran™ 0.2 µm NC, GE Healthcare Life Science, Buckinghamshire, UK). The membrane was blocked and incubated with the primary antibody at 4 °C overnight. After washing thrice with TBS containing 0.1 % Tween-20 (TBS-T), the membranes were incubated with secondary antibodies for 1 h at room temperature.

1.3 Computational simulation

We placed these model systems in a cubic box with dimensions ~8.5 × 8.5 × 8.5 nm^3 and solvated them by adding simple point-charge (SPC) [1, 2] water molecules together with a physiological (150 mM) concentration of NaCl. Afterwards, the systems were energy-minimised using the steepest descent method, followed by a series of equilibration runs with the following positional restraints: (a) positional restraints on the KD backbone atoms, a force constant of 10,000 $kJ.mol^{-1}.nm^{-2}$, and an NVT ensemble (i.e. constant number of particles, volume, and temperature) for 2 ns; (b) the same as in (a) but in an NpT ensemble (i.e. constant number of particles, pressure, and temperature); (c) the same as in (b) but a force constant of 1,000 $kJ.mol^{-1}.nm^{-2}$; and (d) the same as in (b) but a force constant of 200 $kJ.mol^{-1}.nm^{-2}$ for 6 ns. In this manner, we were able to slowly equilibrate the systems without causing strong disturbances in their original structures. Subsequently, we carried out the final equilibration simulations, again using the NpT ensemble for 200 ns (in the case of the native KD) and 750 ns (in the case of the oxidised KD), without any positional restraints.

2. Supplement results

We focused on Met and Cys residues for oxidation of the FAK protein, which are highly reactive amino acids (AAs). However, to find out which of the Met or Cys to oxidize, we calculated the solvent accessible surface area (SASA) of these residues. Thus, based on the SASA results we selected six AAs (i.e., Cys427, Met442, Cys559, Met571, Met617 and Met643) for oxidation, see AAs highlighted with light blue color in Table 1. As is clear, these residues have higher accessibility to solvent. To oxidize the above-mentioned AAs, we modified Met to methionine sulfoxide and Cys to cysteic acid (Figure S1).

Figure S1. Schematic illustration of the native and oxidized kinase domain (KD) of the FAK protein, together with its six amino acids (Met and Cys residues) selected for oxidation. The residues shown in the left and right figure are those before and after oxidation, respectively (see also Table S2).

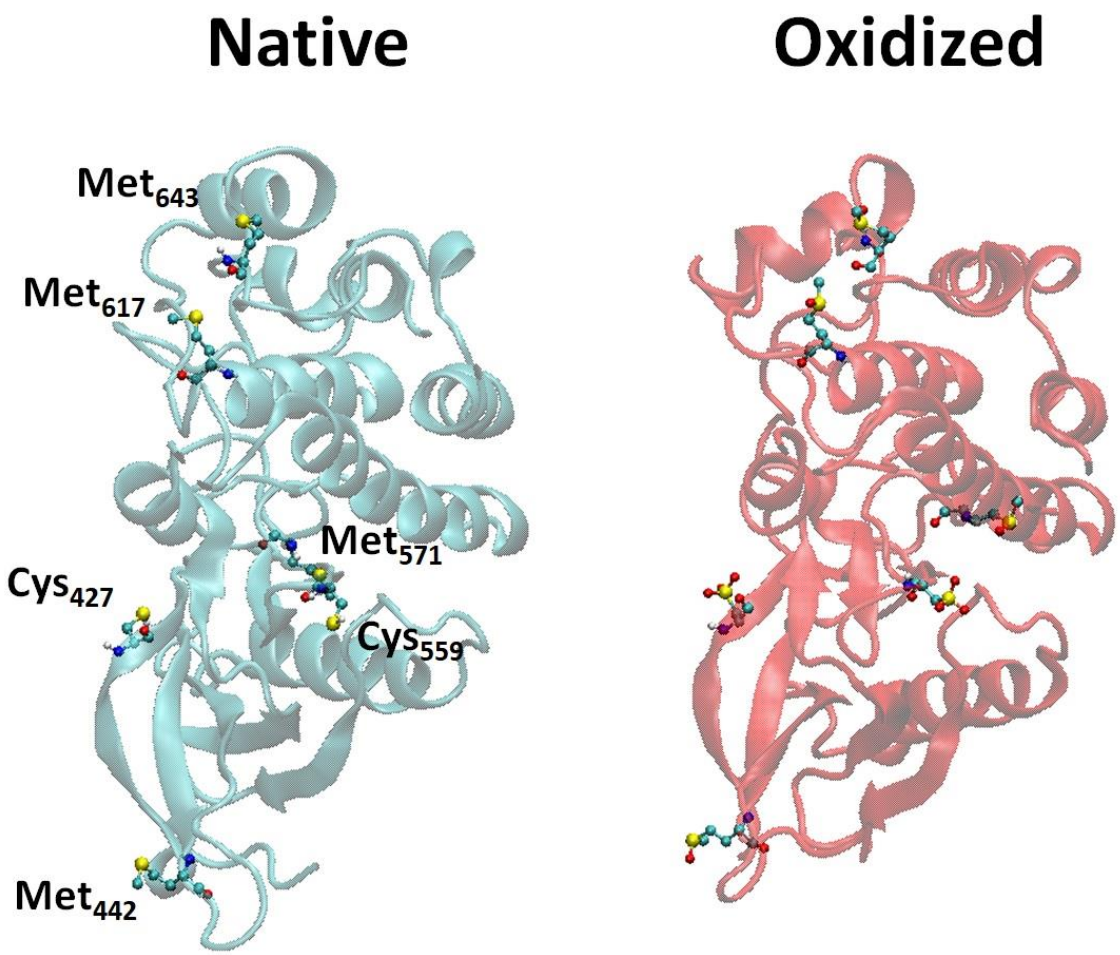

The percentage of the random coil structure increases, and the α-helix structure decreases by approximately 2-3 %, whereas other conformations stay more or less unchanged. This indicates that the oxidation results in a slight increase in the structural flexibility, thereby affecting its stability. Note that the oxidation degree used in our simulations is low, which probably corresponds to a short treatment time. Therefore, it does not lead to drastic conformational changes. However, it is most likely sufficient to change the function of FAK protein, thereby affecting its activity.

Figure S2. A slight conformational change and twisting in the FAK protein after oxidation.

Native

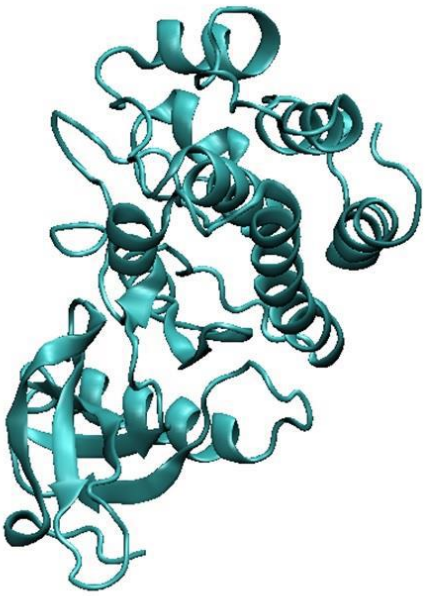

Oxidized

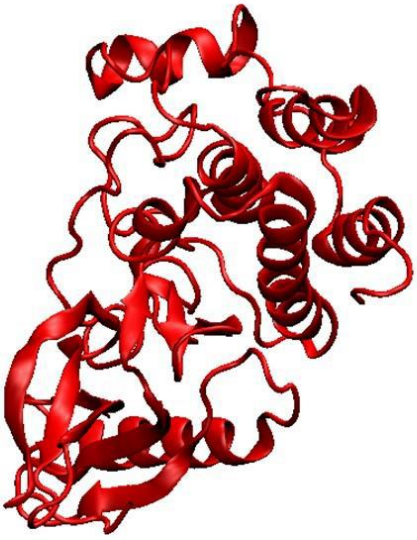

Native

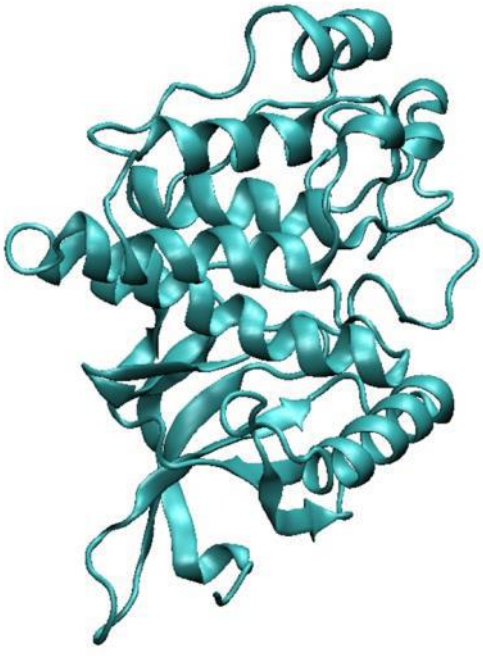

Oxidized

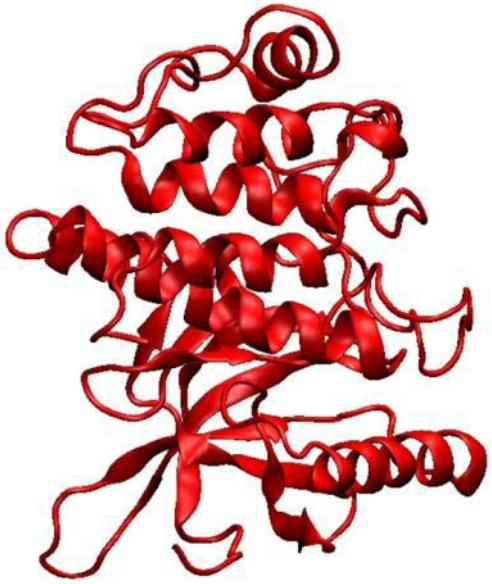

Figure S3. Zymography original blot. Clear areas represent proteolytic activity evaluated for NBP treatment on HGF cells. Lane 1, marker, lane 2, control, lane 3, NBP treated for 3 min.

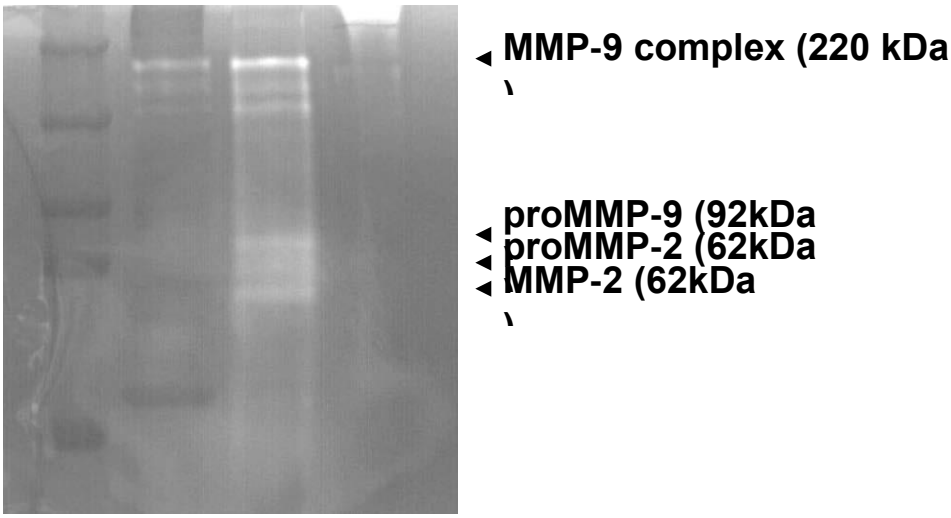

The native FAK reaches its equilibration after ~100 ns and stays stable in the rest of the simulation time, yielding an RMSD fluctuating around 0.43 nm. In contrast, the oxidized FAK protein obtains its stability at a much longer time, i.e., at around 600 ns, having a higher RMSD value than the native one, which fluctuates around 0.55 nm. This indicates that the oxidized structure become slightly more flexible than the native structure, which can be due to the conformational changes in the protein. Indeed, the secondary structure analysis showed a slight difference in secondary structure after oxidation (Table S2).

Table S1. Met and Cys residues of the KD of the FAK protein. Rows highlighted with light blue color show the residues that have higher SASA and are hence chosen for oxidation.

AA residue	Residue number	SASA (nm^2)
CYS	427	0.59 ± 0.14
MET	442	0.94 ± 0.16
CYS	456	0.04 ± 0.04
CYS	459	0.03 ± 0.03

MET	475	0.18 ± 0.10
MET	499	0.05 ± 0.05
CYS	502	0.02 ± 0.02
CYS	559	0.32 ± 0.09
MET	571	0.46 ± 0.16
MET	589	0.04 ± 0.04
MET	607	0.03 ± 0.03
CYS	611	0.02 ± 0.02
MET	612	0.02 ± 0.02
MET	617	0.44 ± 0.09
MET	643	0.99 ± 0.16
CYS	647	0.14 ± 0.08
MET	655	0.00 ± 0.00
CYS	658	0.00 ± 0.00

Table S2. Chemical structures of Met and Cys and their oxidized forms used for the creation of the oxidized KD of the FAK protein.

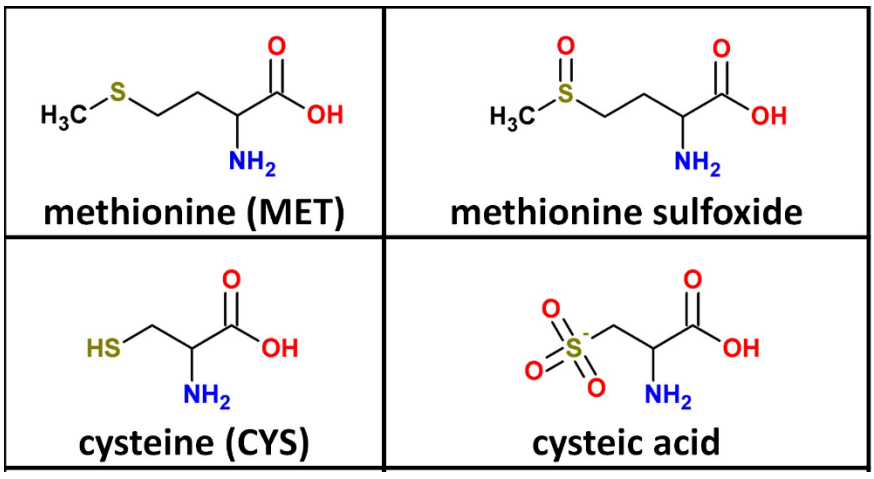

Table S3. Secondary structure analysis of the native and oxidized KD of the FAK protein.

System	Coil	β-sheet	β-bridge	Bend	Turn	α-helix	3-helix
Native	0.22 ± 0.02	0.15 ± 0.00	0.01 ± 0.00	0.13 ± 0.01	0.12 ± 0.01	0.35 ± 0.02	0.02 ± 0.01
Oxidized	0.25 ± 0.01	0.14 ± 0.01	0.01 ± 0.00	0.13 ± 0.01	0.11 ± 0.01	0.33 ± 0.01	0.02 ± 0.01

Reference

1 Berendsen, H. J., Postma, J. P. M., van Gunsteren, W. F. & Hermans, J. Interaction models for water in relation to protein hydration. In Pullman, B. (ed.) *Intermolecular forces*. The Jerusalem Symposia on Quantum Chemistry and Biochemistry, Vol. 14, 331–342 (Springer, 1981).

2. Hermans, J., Berendsen, H. J. C., Van Gunsteren, W. F. & Postma, J. P. M. A consistent empirical potential for water-protein interactions. *Biopolymers* **23,** 1513–1518 (1984).